Copyright © 2010 Tech Science Press CMES, vol.59, no.3, pp.239-274, 2010

A Backward Group Preserving Scheme for Multi-Dimensional Backward Heat Conduction Problems

Chih-Wen Chang[1] **and Chein-Shan Liu**[2]

Abstract: In this article, we propose a backward group preserving scheme (BGPS) to tackle the multi-dimensional backward heat conduction problem (BHCP). The BHCP is well-known as severely ill-posed because the solution does not continuously depend on the given data. When eight numerical examples (including nonlinear and nonhomogeneous BHCP, and Neumann and Robin conditions of homogeneous BHCP) are examined, we find that the BGPS is applicable to the multi-dimensional BHCP. Even with noisy final data, the BGPS is also robust against disturbance. The one-step BGPS effectively reconstructs the initial data from the given final data, which with a suitable grid length produces a highly accurate solution never seen before. The results are very important in the computations of multi-dimensional BHCP.

Keywords: Nonlinear backward heat conduction problem, Strongly ill-posed problem, Nonhomogeneous heat conduction equation, Backward group preserving scheme (BGPS), Group preserving scheme (GPS)

1 Introduction

Heat conduction problems that appear from engineering applications are usually divided into direct heat conduction problems and inverse heat conduction problems. Among the inverse heat conduction problems, the backward heat conduction problems (BHCPs) are the most strongly ill-posed ones since the solution is unstable for any given final data. Many methods have been proposed for solving the homogeneous BHCP, for example, the boundary element method [Han, Ingham and Yuan (1995)], the iterative boundary element method [Mera, Elliott, Ingham and Lesnic (2001); Mera, Elliott and Ingham (2002); Jourhmane and Mera (2002)], the explicit inversion algorithm and the sequential scheme of inversion [Muniz, de

[1] Grid Applied Technology Division, National Center for High-Performance Computing, Taichung 40763, Taiwan. Corresponding author, E-mail: d93510002@ntou.edu.tw
[2] Department of Civil Engineering, National Taiwan University, Taipei 10617, Taiwan

Campos Velho and Ramos (1999)], the Tikhonov regularization, maximum entropy principle and truncated singular value decomposition [Muniz, Ramos and de Campos Velho (2000)], the operator-splitting methods [Kirkup and Wadsworth (2002)], the regularized successive over-relaxation inversion [Liu (2002)], the method of fundamental solutions and the standard Tikhonov regularization technique [Mera (2005)], and the high order lattice-free finite difference method [Iijima (2004)].

Recently, Liu, Chang and Chang (2006) have employed the backward group preserving scheme (BGPS) to tackle the nonhomogeneous BHCP. Lack of need for a priori regularization in use, makes the BGPS more appealing for inverse problems with a final value problem. Actually the BGPS was an extension of the work by Liu (2004) by taking time regression of equations into account in the formation of backward group theory. In the paper of Liu (2004), the group preserving scheme (GPS) was first adopted to deal with the nonhomogeneous BHCP because the GPS [Liu (2001)] was an effective numerical approximation for solving nonlinear differential equations. The BHCP has been solved by using the BGPS [Liu, Chang and Chang (2006)], and the Lie-group shooting method (LGSM) [Chang, Liu and Chang (2007)] to a moderate time span, and Liu (2004) utilized two transformations to resolve BHCPs; nevertheless, he did not consider how the final time data were affected by noises. Later, Liu, Chang and Chang (2006) proposed an explicit single-step algorithm to resolve BHCPs, but they could not tackle the BHCPs with time varying boundary conditions very well when there were noisy final data. Recently, Chang, Liu and Chang (2007) and Chang, Liu and Chang (2009) have used the numerical implementation of quasi-reversibility together with the time-direction LGSM to solve the BHCP and obtained good results. Besides, Chang, Liu and Chang (2010a) and Chang, Liu and Chang (2010b) used the quasi-boundary semi-analytical approach to tackle BHCPs and achieved nearly exact solutions. A recent review of the numerical BHCP was provided by Chiwiacowsky and de Campos Velho (2003).

For the multi-dimensional nonlinear and nonhomogeneous BHCPs, Long and Dinh (1994) proposed the regularization method to tackle the nonlinear BHCP, but its maximum error is quite large over 0.2. After that, Feng, Qian and Fu (2008) used the Tikhonov regulization method to deal with the nonhomogeneous BHCP. However, this approach did not give good results even with a small final time $T = 0.1$. Later, the quasi-reversibility method for the nonhomogeneous BHCP was employed by Trong and Tuan (2006). Although the approach gave good results, the retrieved time $T = 0.5$ is still small. Nevertheless, Trong and Tuan (2009a) used a method of integral equation to resolve the nonlinear BHCP, and they reported that regularized results are better than their previous results [Trong, Quan, Khanh and Tuan (2007); Trong and Tuan (2008b)]. Apart from this, Trong and Tuan (2008a)

proposed a simple and convenient regularization method to tackle the nonhomogeneous BHCP. However, they claimed that the regularized results are better than their previous results [Trong and Tuan (2006)]. For the two-dimensional (2-D) BHCP, Trong and Tuan (2009b) employed a truncated Fourier series method to solve the 2-D nonlinear BHCP, but this approach was complicated. After that, Tuan and Trong (2009) adopted a new regularized method to deal with the 2-D nonhomogeneous BHCP.

The BHCP is unlike the sideways heat conduction problem recently reviewed and calculated by Chang, Liu and Chang (2005). The degree of the ill-posedness of BHCP is greater than that of the sideways heat conduction problem, which is coped with by the reconstruction of unknown boundary conditions.

The present paper is organized as follows. Section 2 illustrates the multi-dimensional nonlinear and nonhomogeneous BHCP and its final condition, boundary conditions and semi-discretization. We give a sketch of the GPS for ordinary differential equations (ODEs) and derive the BGPS [Liu, Chang and Chang (2006); Liu (2006); Liu, Chang and Chang (2010)] for the backward differential equations system in Section 3. In Section 4, we employ the semi-discretization and a one-step BGPS to solve some numerical examples. Finally, we draw some conclusions in Section 5.

2 Backward heat conduction problems

The multi-dimensional nonlinear and nonhomogeneous BHCP we ponder is respectively given by the following equations:

$$\frac{\partial u}{\partial t} = \gamma \Delta u + F(u) + f \text{ in } \Omega, \tag{1}$$

$$u = u_B \text{ on } \Gamma_{\mathrm{B}}, \tag{2}$$

$$u = u_F \text{ on } \Gamma_{\mathrm{F}}, \tag{3}$$

where u is a scalar temperature field of heat distribution, $F(u)$ is a nonlinear function of u, and f is the heat source. We take a bounded domain D in R^j, $j = 1,2,3$ and a spacetime domain $\Omega = D \times (0,T)$ in R^{j+1} for a final time $T > 0$, and write two surfaces $\Gamma_{\mathrm{B}} = \partial D \times [0,T]$ and $\Gamma_{\mathrm{F}} = \partial D \times \{T\}$ of the boundary $\partial\Omega$. Δ represents the j-dimensional Laplacian operator. While Eqs. (1)-(3) constitute a j-dimensional backward heat conduction problem for a given boundary data u_B: $\Gamma_{\mathrm{B}} \mapsto R$ and a final data u_F: $\Gamma_{\mathrm{F}} \mapsto R$.

Applying a semi-discrete procedure to Eq. (1), yields a coupled system of ODEs:

$$\dot{u}_{i,j,k}(t) - \gamma \left\{ \frac{[u_{i+1,j,k}(t) - 2u_{i,j,k}(t) + u_{i-1,j,k}(t)]}{(\Delta x)^2} \right.$$

$$+\frac{[u_{i,j+1,k}(t)-2u_{i,j,k}(t)+u_{i,j-1,k}(t)]}{(\Delta y)^2}$$
$$+\frac{[u_{i,j,k+1}(t)-2u_{i,j,k}(t)+u_{i,j,k-1}(t)]}{(\Delta z)^2}\Bigg\}-F(u_{i,j,k})=f_{i,j,k}(t), \tag{4}$$

where $\Delta x, \Delta y$ and Δz are uniform spatial lengths in x, y and z directions, $u_{i,j,k}(t) = u(i\Delta x, j\Delta y, k\Delta z, t), f_{i,j,k}(t) = f(i\Delta x, j\Delta y, k\Delta z, t, u(i\Delta x, j\Delta y, k\Delta z, t))$, and $\dot{u}$ denotes the differential of u with respect to t. Obviously, in Eq. (4) there are totally n^3 coupled nonlinear differential equations for the n^3 variables $u_{i,j,k}(t)$, $i, j, k = 1, 2, \cdots, n$, which, even for a specified final time condition can be numerically integrated by the BGPS developed in Section 3.2 for the resulting backward ODEs.

3 Numerical methods

We will divide problems and solvers into two classes: section 3.1 Forward problems and group preserving scheme, and section 3.2 Backward problems and backward group preserving scheme.

3.1 Forward problems and Group preserving scheme

3.1.1 Dynamics on a future cone

GPS can preserve the internal symmetry group of the considered system. For nonlinear differential equations systems, Liu (2001) has embedded them into the augmented dynamical systems, which concern with not only the evolution of state variables but also the evolution of the magnitude of state variables vector. That is, for an n ordinary differential equations system:

$$\dot{\mathbf{x}} = \mathbf{f}(\mathbf{x}, t),\ \mathbf{x} \in \mathbb{R}^n,\ t \in \mathbb{R}^+, \tag{5}$$

we can embed it into the following n+1-dimensional augmented dynamical system:

$$\frac{d}{dt}\begin{bmatrix}\mathbf{x}\\ \|\mathbf{x}\|\end{bmatrix} = \begin{bmatrix}0_{n\times n} & \frac{\mathbf{f}(\mathbf{x},t)}{\|\mathbf{x}\|}\\ \frac{\mathbf{f}^{\mathrm{T}}(\mathbf{x},t)}{\|\mathbf{x}\|} & 0\end{bmatrix}\begin{bmatrix}\mathbf{x}\\ \|\mathbf{x}\|\end{bmatrix}. \tag{6}$$

Here, we assume $\|\mathbf{x}\| > 0$ and hence, the above system is well-defined.

It is obvious that the first row in Eq. (6) is the same as the original Eq. (5), but the inclusion of the second row in Eq. (6) gives us a Minkowskian structure of the augmented state variables of $\mathbf{X} := (\mathbf{x}^{\mathrm{T}}, \|\mathbf{x}\|)^{\mathrm{T}}$ satisfying a future cone condition as shown in Fig. 1:

$$\mathbf{X}^{\mathrm{T}}\mathbf{g}\mathbf{X} = 0, \tag{7}$$

where

$$\mathbf{g} = \begin{bmatrix} \mathbf{I}_n & \mathbf{0}_{n\times 1} \\ \mathbf{0}_{1\times n} & -1 \end{bmatrix} \tag{8}$$

is a Minkowski metric. $\mathbf{I}_n$ is the identity matrix of order n, and the superscript T denotes the transpose. In terms of $(\mathbf{x}^{\mathrm{T}}, \|\mathbf{x}\|)$, Eq. (7) holds, as

$$\mathbf{X}^{\mathrm{T}}\mathbf{g}\mathbf{X} = \mathbf{x}\cdot\mathbf{x} - \|\mathbf{x}\|^2 = \|\mathbf{x}\|^2 - \|\mathbf{x}\|^2 = 0, \tag{9}$$

where the dot between two n-dimensional vectors represents their Euclidean inner product. The cone condition is thus the most natural constraint that we can impose on the dynamical system (6).

Consequently, we have an n+1-dimensional augmented system:

$$\dot{\mathbf{X}} = \mathbf{A}\mathbf{X} \tag{10}$$

with a constraint (7), where

$$\mathbf{A} := \begin{bmatrix} \mathbf{0}_{n\times n} & \frac{\mathbf{f}(\mathbf{x},t)}{\|\mathbf{x}\|} \\ \frac{\mathbf{f}^{\mathrm{T}}(\mathbf{x},t)}{\|\mathbf{x}\|} & 0 \end{bmatrix} \tag{11}$$

is an element of the Lie algebra $so(n,1)$ of the proper orthochronous Lorentz group $SO_o(n,1)$, satisfying

$$\mathbf{A}^{\mathrm{T}}\mathbf{g} + \mathbf{g}\mathbf{A} = 0. \tag{12}$$

This fact prompts us to employ the group preserving scheme, and its discretized mapping $\mathbf{G}$ exactly preserves the following properties:

$$\mathbf{G}^{\mathrm{T}}\mathbf{g}\mathbf{G} = \mathbf{g}, \tag{13}$$

$$det\mathbf{G} = 1, \tag{14}$$

$$G_0^0 > 0, \tag{15}$$

where G_0^0 is the 00th component of $\mathbf{G}$. Such $\mathbf{G}$ is an element of $SO_o(n,1)$. The term orthochronous should be understood as the preservation of the sign of $\|\mathbf{x}\| > 0$. The discretization procedure will be presented depending on each problem after this section.

Remarkably, the original n-dimensional dynamical system (5) in the usual Euclidean space $\mathbb{E}^n$ can be embedded very naturally into an augmented n+1-dimensional

dynamical system (10) in the Minkowski space $\mathbb{M}^{n+1}$ and these two systems are mathematically equivalent. Although the dimension of the new system rises by one, Liu (2001) has shown that, under the Lipschitz condition of

$$\|\mathbf{f}(\mathbf{x},t)-\mathbf{f}(\mathbf{y},t)\| \leq \mathscr{L}\|\mathbf{x}-\mathbf{y}\|, \ \forall(\mathbf{x},t),(\mathbf{y},t) \in \mathbf{D}, \tag{16}$$

where $\mathbf{D}$ is a domain in $\mathbb{R}^n \times \mathbb{R}^+$, and $\mathscr{L}$ is known as a Lipschitz constant, the new system has the advantage of admitting a group preserving numerical scheme as follows:

$$\mathbf{X}_{\ell+1} = \mathbf{G}(\ell)\mathbf{X}_\ell, \tag{17}$$

where $\mathbf{X}_\ell$ stands for the numerical evaluation of $\mathbf{X}$ at the discrete time t_ℓ, and $\mathbf{G}(\ell) \in SO_o(n,1)$ is the group evaluation at time t_ℓ.

3.1.2 GPS for forward differential equations system

To give a step by step numerical scheme, we suppose that $\mathbf{A}(\ell)$ in Eq. (10) is a constant matrix, taking its value at the l-th step. An exponential mapping of $\mathbf{A}(\ell)$ for the interval $t_\ell \leq t < t_\ell + \Delta t$, when the time parameter t in Eq. (11) is approximately fixed as $t = t_\ell$, admits:

$$\exp[\Delta t\mathbf{A}(\ell)] = \begin{bmatrix} \mathbf{I}_n + \frac{(a_\ell-1)}{\|\mathbf{f}_\ell\|^2}\mathbf{f}_\ell\mathbf{f}_l^{\mathrm{T}} & \frac{b_\ell \mathbf{f}_\ell}{\|\mathbf{f}_\ell\|} \\ \frac{b_\ell \mathbf{f}_l^{\mathrm{T}}}{\|\mathbf{f}_\ell\|} & a_\ell \end{bmatrix}, \tag{18}$$

where

$$a_\ell := \cosh\left(\frac{\Delta t\|\mathbf{f}_\ell\|}{\|\mathbf{x}_\ell\|}\right), \ b_\ell := \sinh\left(\frac{\Delta t\|\mathbf{f}_\ell\|}{\|\mathbf{x}_\ell\|}\right). \tag{19}$$

For saving notation, we use $\mathbf{f}_\ell = \mathbf{f}(\mathbf{x}_\ell, t_\ell)$. Substituting the above $exp[\Delta t\mathbf{A}(\ell)]$ for $\mathbf{G}(\ell)$ into Eq. (17) and taking its first row, we obtain

$$\mathbf{x}_{l+1} = x_\ell + \frac{(a_\ell-1)\mathbf{f}_\ell\cdot\mathbf{x}_\ell + b_\ell\|\mathbf{x}_\ell\|\|\mathbf{f}_\ell\|}{\|\mathbf{f}_\ell\|^2}\mathbf{f}_\ell = \mathbf{x}_\ell + \eta_\ell\mathbf{f}_\ell. \tag{20}$$

From $\mathbf{f}_\ell\cdot\mathbf{x}_\ell \geq -\|\mathbf{f}_\ell\|\|\mathbf{x}_\ell\|$, we can prove that

$$\eta_\ell \geq \left[1-\exp\left(-\frac{\Delta t\|\mathbf{f}_\ell\|}{\|\mathbf{x}_\ell\|}\right)\right]\frac{\|\mathbf{x}_\ell\|}{\|\mathbf{f}_\ell\|} > 0, \ \forall\Delta t > 0. \tag{21}$$

This scheme is group properties preserved for all $\Delta t > 0$.

3.2 Backward problems and backward group preserving scheme

3.2.1 Dynamics on a past cone

Corresponding to the initial value problems governed by Eq. (5) with a specified initial value $\mathbf{x}(0)$ at an initial time, for many systems in the engineering applications, the final value problems may happen because one wants to retrieve the past histories of state variables exhibited in the physical models. These time backward problems of ordinary differential equations type can be described by

$$\dot{\mathbf{x}} = \mathbf{f}(\mathbf{x},t),\ \mathbf{x} \in \mathbb{R}^n,\ t \in \mathbb{R}^-. \tag{22}$$

With a specified final value $\mathbf{x}(0)$ at $t = 0$, we intend to recover the past values of $\mathbf{x}$ in the past time of $t < 0$.

We can embed Eq. (22) into the following n+1-dimensional augmented dynamical system:

$$\frac{d}{dt}\begin{bmatrix} \mathbf{x} \\ -\|\mathbf{x}\| \end{bmatrix} = \begin{bmatrix} \mathbf{0}_{n\times n} & -\frac{\mathbf{f}(\mathbf{x},t)}{\|\mathbf{x}\|} \\ -\frac{\mathbf{f}^{\mathrm{T}}(\mathbf{x},t)}{\|\mathbf{x}\|} & 0 \end{bmatrix} \begin{bmatrix} \mathbf{x} \\ -\|\mathbf{x}\| \end{bmatrix}. \tag{23}$$

It is obvious that the first row in Eq. (23) is the same as the original Eq. (22), but the inclusion of the second row in Eq. (6) gives us a Minkowskian structure of the augmented state variables of $\mathbf{X} := (\mathbf{x}^{\mathrm{T}}, -\|\mathbf{x}\|)^{\mathrm{T}}$ satisfying a past cone condition:

$$\mathbf{X}^{\mathrm{T}}\mathbf{g}\mathbf{X} = \mathbf{x}\cdot\mathbf{x} - \|\mathbf{x}\|^2 = \|\mathbf{x}\|^2 - \|\mathbf{x}\|^2 = 0. \tag{24}$$

Here, we should stress that the cone condition imposed on the dynamical system (6) is a future cone as shown in Fig. 1, while that for the dynamical system (23) the cone condition (24) imposed is a past cone as shown in Fig. 1.

Consequently, we have an n+1-dimensional augmented system:

$$\dot{\mathbf{X}} = \mathbf{B}\mathbf{X} \tag{25}$$

with a constraint (24), where

$$\mathbf{B} := \begin{bmatrix} \mathbf{0}_{n\times n} & -\frac{\mathbf{f}(\mathbf{x},t)}{\|\mathbf{x}\|} \\ -\frac{\mathbf{f}^{\mathrm{T}}(\mathbf{x},t)}{\|\mathbf{x}\|} & 0 \end{bmatrix}, \tag{26}$$

satisfying

$$\mathbf{B}^{\mathrm{T}}\mathbf{g} + \mathbf{g}\mathbf{B} = 0, \tag{27}$$

which is a Lie algebra $so(n,1)$ of the proper orthochronous Lorentz group $SO_o(n,1)$. The term orthochronous used here is referred to the preservation of the sign of $-\|\mathbf{x}\| < 0$.

According to the above Lie algebra property of $\mathbf{B}$, we can derive a backward group preserving scheme as Eq. (17) for Eq. (10):

$$\mathbf{X}_{\ell-1} = \mathbf{G}(\ell)\mathbf{X}_\ell. \tag{28}$$

The above is a backward single-step numerical scheme. Below we derive a group preserving scheme for Eq. (25).

3.2.2 BGPS for backward differential equations system

Similarly, by assuming that $\mathbf{B}(\ell)$ is a constant matrix, an exponential mapping of $\mathbf{B}(\ell)$ admits a closed-form representation:

$$\exp[-\Delta t\mathbf{B}(\ell)] = \begin{bmatrix} \mathbf{I}_n + \frac{(a_\ell-1)}{\|\mathbf{f}_\ell\|^2}\mathbf{f}_\ell\mathbf{f}_l^{\mathrm{T}} & \frac{b_\ell\mathbf{f}_\ell}{\|\mathbf{f}_\ell\|} \\ \frac{b_\ell\mathbf{f}_l^{\mathrm{T}}}{\|\mathbf{f}_\ell\|} & a_\ell \end{bmatrix}, \tag{29}$$

where a_ℓ and b_ℓ are still defined by Eq. (19).

Substituting the above $\exp[-\Delta t\mathbf{B}(\ell)]$ for $\mathbf{G}(\ell)$ into Eq. (28) and taking its first row, we obtain

$$\mathbf{x}_{\ell-1} = \mathbf{x}_\ell + \frac{(a_\ell-1)\mathbf{f}_\ell\cdot\mathbf{x}_\ell - b_\ell\|\mathbf{x}_\ell\|\ \|\mathbf{f}_\ell\|}{\|\mathbf{f}_\ell\|^2}\mathbf{f}_\ell = \mathbf{x}_\ell + \eta_\ell\mathbf{f}_\ell. \tag{30}$$

From $\mathbf{f}_\ell\cdot\mathbf{x}_\ell \le \|\mathbf{f}_\ell\|\ \|\mathbf{x}_\ell\|$, we can prove that

$$\eta_\ell \le \left[\exp\left(-\frac{\Delta t\,\|\mathbf{f}_\ell\|}{\|\mathbf{x}_\ell\|}\right) - 1\right]\frac{\|\mathbf{x}_\ell\|}{\|\mathbf{f}_\ell\|} < 0,\ \forall\Delta t > 0. \tag{31}$$

This scheme is group properties preserved for all $\Delta t > 0$.

Comparing Eqs. (30) with (20), we note that they have the same form except that the sign before $b_\ell\|\mathbf{x}_\ell\|\ \|\mathbf{f}_\ell\|$ in the numerators. We will call this numerical scheme a backward group preserving scheme (BGPS), which is slightly different from the group preserving scheme (GPS) introduced in Section 3.2.1 for the forward differential dynamics.

4 Numerical examples

We will apply the BGPS to the calculations of BHCP through numerical examples. We are interested in the stability of our approach when the input final measured data

are polluted by random noise for different problems. We can evaluate the stability by increasing the different levels of random noise in the final data:

$$\hat{\mathbf{u}}_{\mathrm{F}} = \mathbf{u}_{\mathrm{F}} + s[2R(i) - 1], \tag{32}$$

where $\mathbf{u}_{\mathrm{F}}$ is the final exact data, respectively. We use the function RANDOM_NUMBER given in Fortran to generate the noisy data $R(i)$, which are random numbers in [-1, 1], and s means the level of absolute noise. Then, the final noisy data $\hat{\mathbf{u}}_{\mathrm{F}}$ are employed in the calculations. Usually, when the exact data is small, we use the relative random noise to represent noise

$$s_r = \frac{s}{\left|\mathbf{u}_{\mathrm{F}}^{\max}\right|} \times 100\%, \tag{33}$$

where $\mathbf{u}_{\mathrm{F}}^{\max}$ is the maximum exact data.

4.1 Example 1

Consider the following one-dimensional homogeneous BHCP:

$$u_t = \gamma u_{xx},\ 0 < x < \pi,\ 0 < t < T, \tag{34}$$

with the Robin boundary condition

$$u_x(0,t) = u_x(\pi,t) + u(\pi,t) = 0, \tag{35}$$

and the initial condition

$$u(x,0) = cos(5x). \tag{36}$$

Here, the final data is calculated by the GPS with a time increment $\Delta t = 0.001$ and a grid length $\Delta x = \pi/100$:

$$g(x) = u(x,T),\ T > t \geq 0. \tag{37}$$

In the literature, this one-dimensional BHCP often arose in the area of archeology [Li and Liu (2005)]. For this computational example, we have taken $\gamma = 0.01$, $T =$ 0.5, 1 and 5, and calculated this example by the one-step BGPS. The accuracy as can be seen from Fig. 2(a) is rather good. Li and Liu (2005) have calculated this example by the Morozov discrepancy principle and shown that this method does not give satisfactory results with terminal times T = 0.5, 1, 5 as shown in their Figure 3.

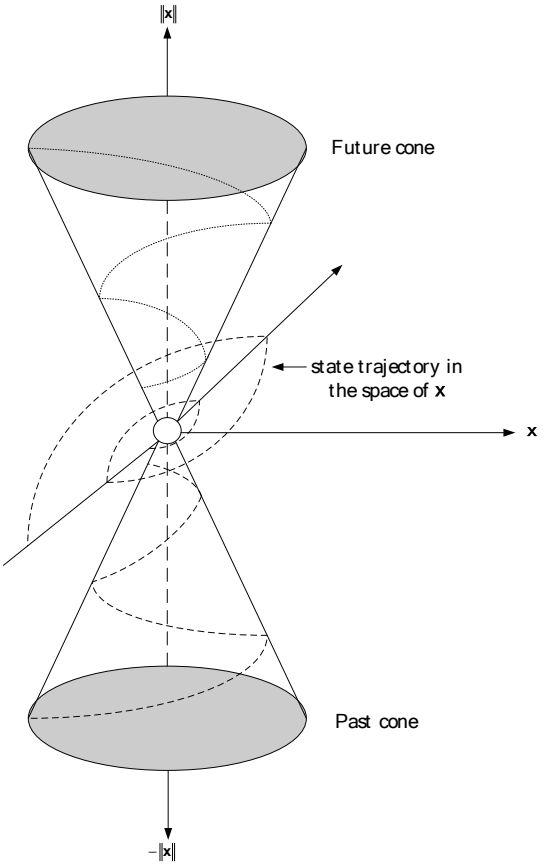

Figure 1: The construction of deleted cones in the Minkowski space for forward and backward problems signifies a conceptual breakthrough. The trajectory observed in the state space $\mathbf{x}$ is a parallel projection of the trajectory in the null cones along the $\|\mathbf{x}\|$ or $-\|\mathbf{x}\|$-axis.

In this example, when the input final measured data are polluted by random noise, we are concerned about the stability of BGPS, which is investigated by adding the level of random noise on the final data. The results of $T = 0.5$ are compared with the numerical result without considering the relative random noise in Fig. 3. Note that the relative noise level with $s_r = 0.2\%$ disturbs the numerical solutions a little from that without adding the noise.

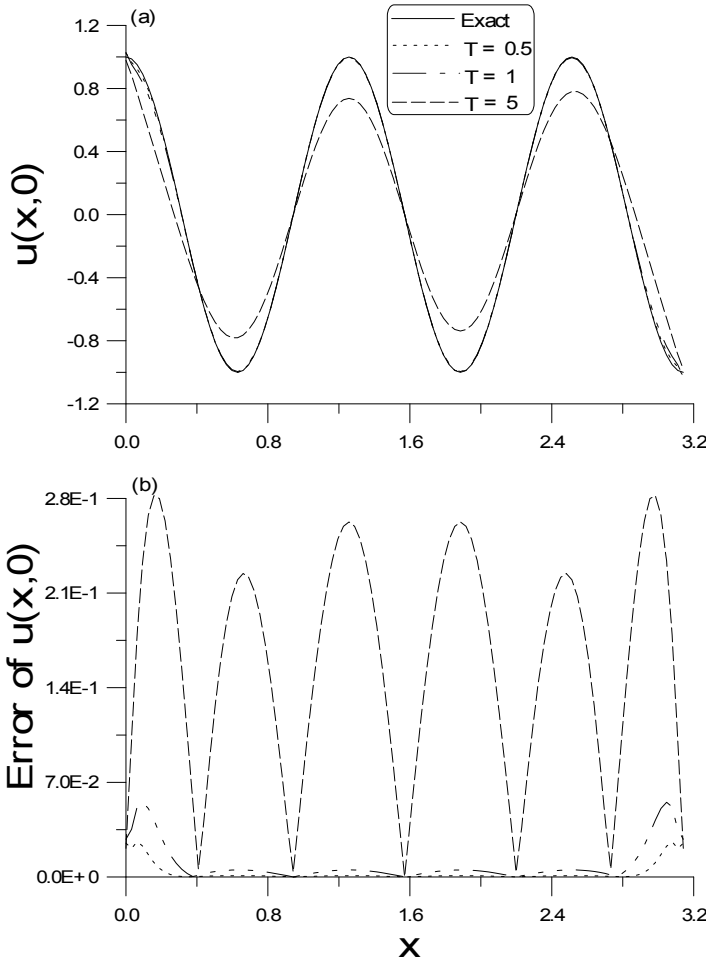

Figure 2: Comparisons of the exact solutions and numerical solutions with final times $T = 0.5$, 1, 5, and the corresponding numerical errors.

4.2 Example 2

The following one-dimensional homogeneous BHCP is considered:

$$u_t = u_{xx},\ 0 < x < \pi,\ 0 < t < T, \tag{38}$$

with the Neumann boundary conditions

$$u_x(0,t) = u_x(\pi,t) = 0, \tag{39}$$

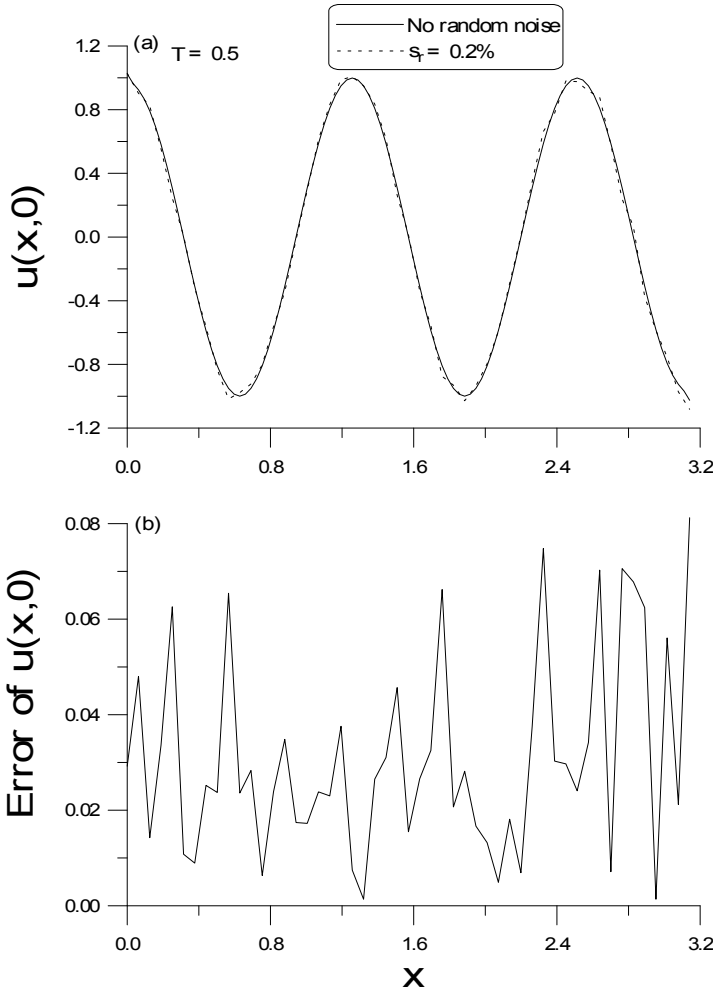

Figure 3: Comparisons of numerical solutions were made in (a) with different levels of noise s_r = 0, 0.2%, and (b) the corresponding numerical errors.

and the final time condition

$$u(x,T) = e^{-T} cos(x). \tag{40}$$

The data to be retrieved is given by

$$u(x,t) = e^{-t} cos(x),\ 0 \le t < T. \tag{41}$$

Fig. 4 demonstrates the numerical results and numerical errors for the final time

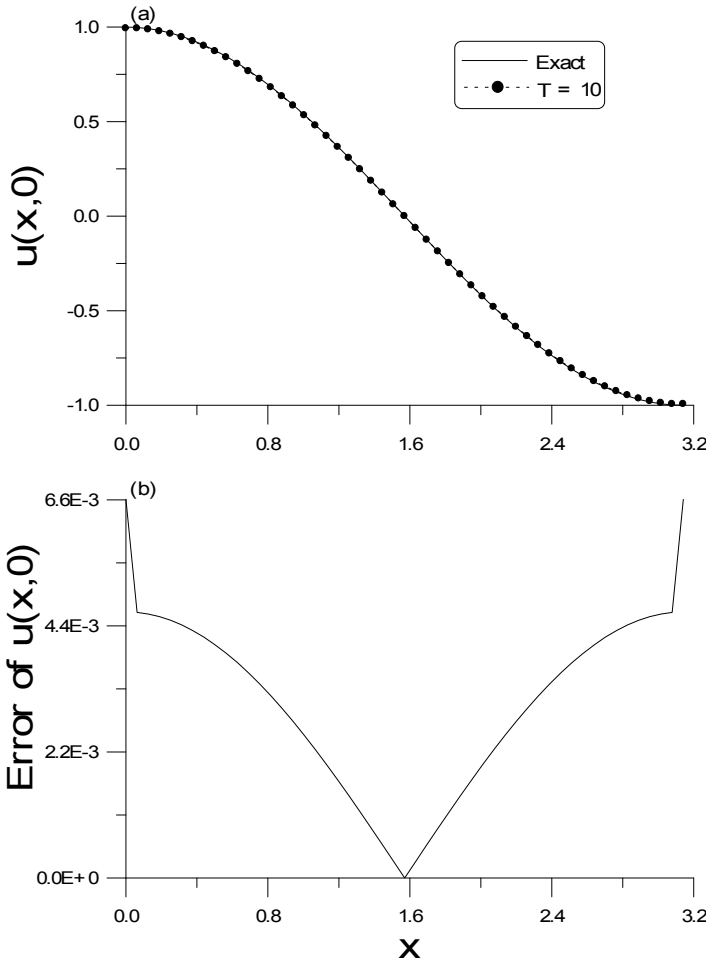

Figure 4: Comparisons of the exact solutions and numerical solutions with the final time $T = 10$, and the corresponding numerical errors.

of $T = 10$ is in the order of $O(10^{-5})$. We attempt to use the BGPS to retrieve the desired initial data of cosx, which are in the order of $O(1)$. The final time of Example 2 is calculated by the BGPS with one step but keeps $\Delta x = 1/200$. Upon comparing with the numerical results of $T = 0.005$ in Li and Liu (2005) with that from the Morozov discrepancy principle, we can say that the BGPS is much better than the Morozov discrepancy principle.

The results under noise are compared with the numerical result without considering the relative random noise in Fig. 5(a). The numerical errors are presented in Fig.

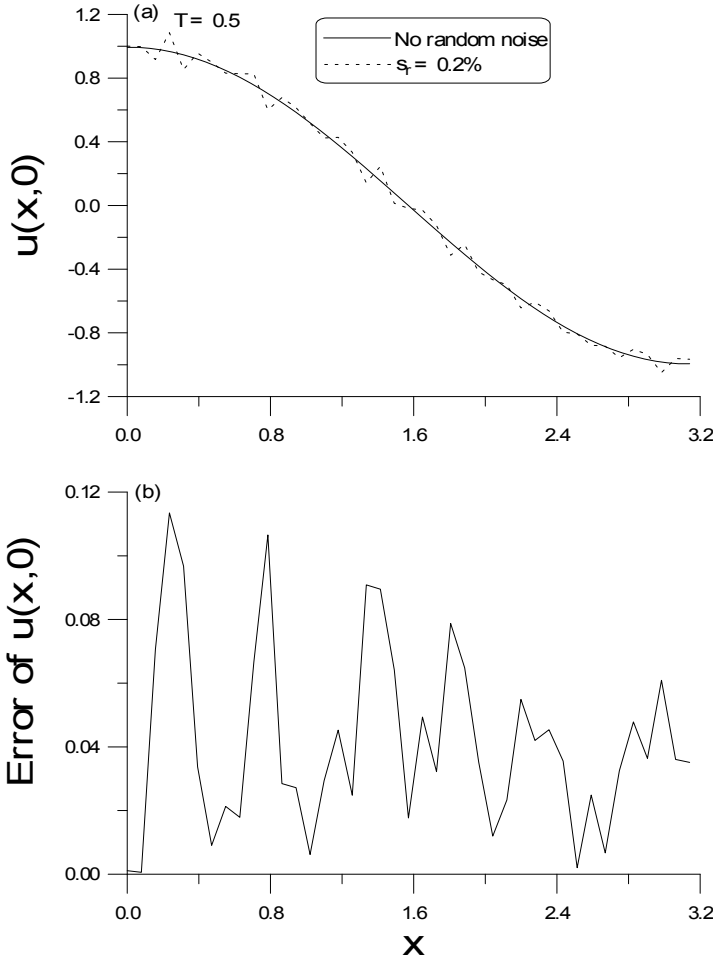

Figure 5: Comparisons of numerical solutions were made in (a) with different levels of noise $s_r = 0$, 0.2%, and (b) the corresponding numerical errors.

5(b), which are smaller than 0.12. Note that the relative noise level with $s_r = 0.2\%$ disturbs the numerical solutions a little from that without considering the noise.

4.3 Example 3

The following one-dimensional nonhomogeneous BHCP is considered:

$$u_t = u_{xx} + 2e^t sin(x),\ 0 < x < \pi,\ 0 < t < T, \tag{42}$$

with the boundary conditions

$$u(0,t) = u(\pi,t) = 0, \tag{43}$$

and the final time condition

$$u(x,T) = e^{\mathrm{T}} sin(x). \tag{44}$$

The data to be retrieved is given by

$$u(x,t) = e^{t} sin(x),\ 0 \le t < T. \tag{45}$$

Fig. 6 presents the numerical results and numerical errors for the final time of T = 10. The final time of Example 3 is also calculated by the BGPS with one step but keeping Δx = 1/75. Upon comparing with the numerical results in [Trong and Tuan (2006); Trong and Tuan (2008a)] with that from the quasi-reversibility method (see Table 1 of the above cited papers), we can say that the BGPS does not need to use the regularization technique and still obtain good results.

In the case, adding a relative noise with level s_r = 0.2% on the input final data, we plotted the numerical result in Fig. 7(a) by the dotted line. Note that the accuracy is still better than the order of 10^{-1} even under a disturbance.

4.4 Example 4

Let us consider another one-dimensional nonhomogeneous BHCP:

$$u_t = u_{xx} - 2e^{-(x+t)},\ 0 < x < \pi,\ 0 < t < T, \tag{46}$$

with the time varying boundary conditions

$$u(0,t) = e^{-t},\ u(\pi,t) = e^{-(\pi+t)}, \tag{47}$$

and the final time condition

$$u(x,T) = e^{-(x+T)}. \tag{48}$$

The exact solution is given by

$$u(x,t) = e^{-(x+t)}. \tag{49}$$

Fig. 8 shows the numerical results and numerical errors for the final time of T = 10. The final time of Example 4 is also calculated by the BGPS with one step but

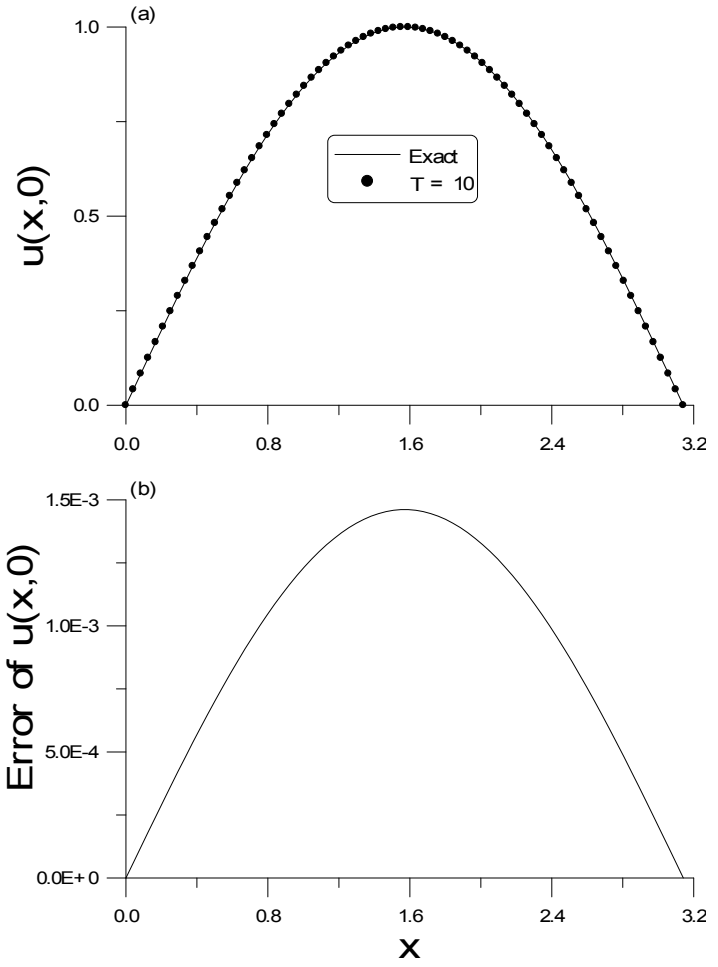

Figure 6: Comparisons of the exact solutions and numerical solutions with the final time $T = 10$, and the corresponding numerical errors.

keeping $\Delta x = 1/90$. Upon comparing with the numerical results of $T = 0.1$ in [Feng, Qian and Fu (2008)] with that from the Tikhonov regularization method (see Figs. 4 and 5 of the above cited paper), we can say that the BGPS does not require to employ the regularization technique and still attain good results.

In the instance, adding a relative noise with level $s_r = 0.6\%$ on the input final data, we plotted the numerical result in Fig. 9(a) by the dotted line. Note that the accuracy is still better than [Feng, Qian and Fu (2008)] even under a disturbance.

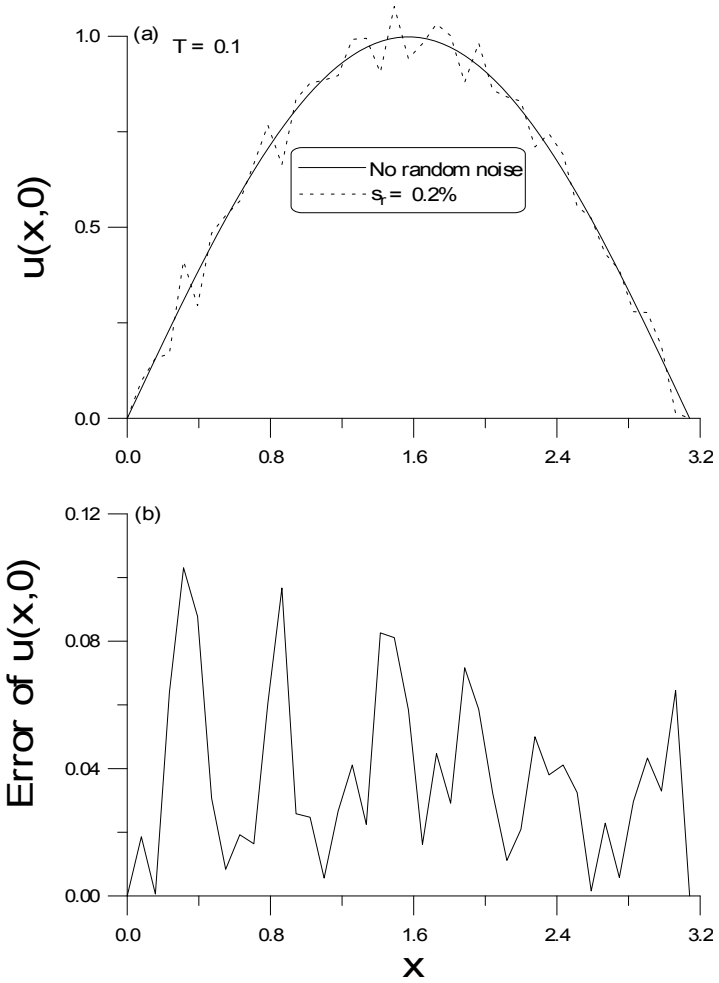

Figure 7: Comparisons of numerical solutions were made in (a) with different levels of noise $s_r = 0, 0.2\%$, and (b) the corresponding numerical errors.

4.5 Example 5

The following one-dimensional nonlinear BHCP is considered:

$$u_t = u_{xx} + F(u) + 2e^t sin(x) - e^{4t} sin^4(x),\ 0 < x < \pi, 0 < t < T, \tag{50}$$

with the boundary conditions

$$u(0,t) = u(\pi,t) = 0, \tag{51}$$

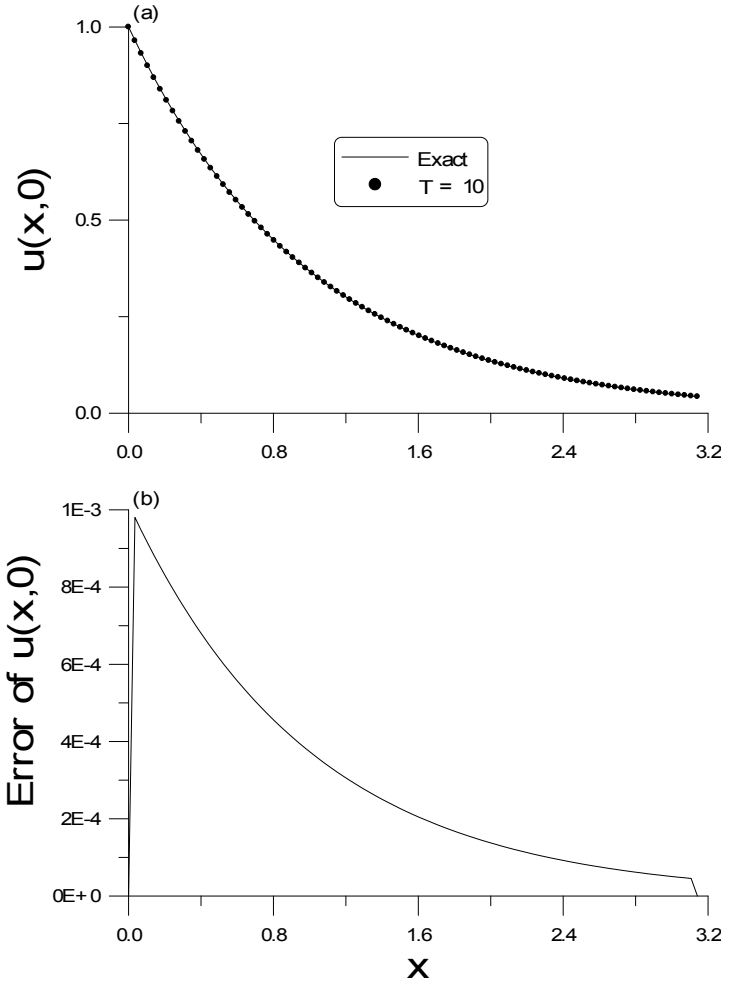

Figure 8: Comparisons of the exact solutions and numerical solutions with the final time $T = 10$, and the corresponding numerical errors.

and the final time condition

$$u(x,T) = e^{\mathrm{T}} sin(x), \tag{52}$$

where $F(u) = \begin{cases} u^4 \ u \in [-e^{10},\ e^{10}] \\ \frac{-e^{10}}{e^{-1}} u + \frac{e^{41}}{e^{-1}} \ u \in (e^{10},\ e^{11}] \\ \frac{e^{10}}{e^{-1}} u + \frac{e^{41}}{e^{-1}} \ u \in (-e^{11},\ -e^{10}] \\ 0 \ |u| > e^{11} \end{cases}$.

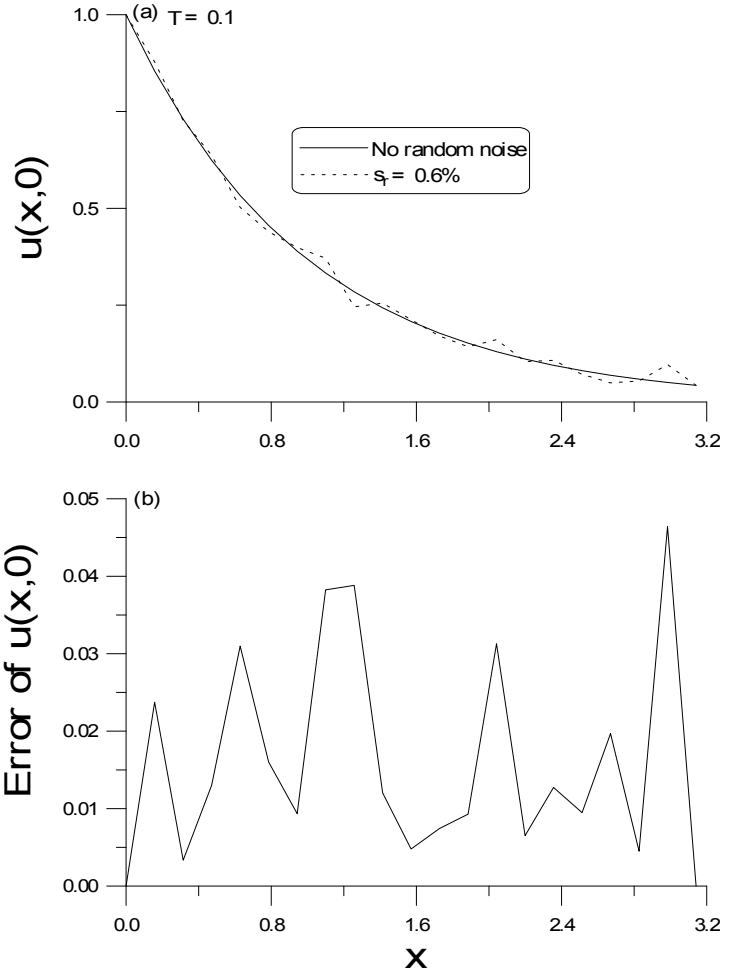

Figure 9: Comparisons of numerical solutions were made in (a) with different levels of noise $s_r = 0, 0.6\%$, and (b) the corresponding numerical errors.

The data to be retrieved is given by

$$u(x,t) = e^t sin(x),\ 0 \le t < T. \tag{53}$$

Fig. 10 displays the numerical results and numerical errors for the final time of T = 1. This example is also calculated by the BGPS with one step but keeping Δx = 1/295. Upon comparing with the numerical results in [Trong and Tuan (2009a)] with that from the method of integral equation (see Table 2 of the above cited pa-

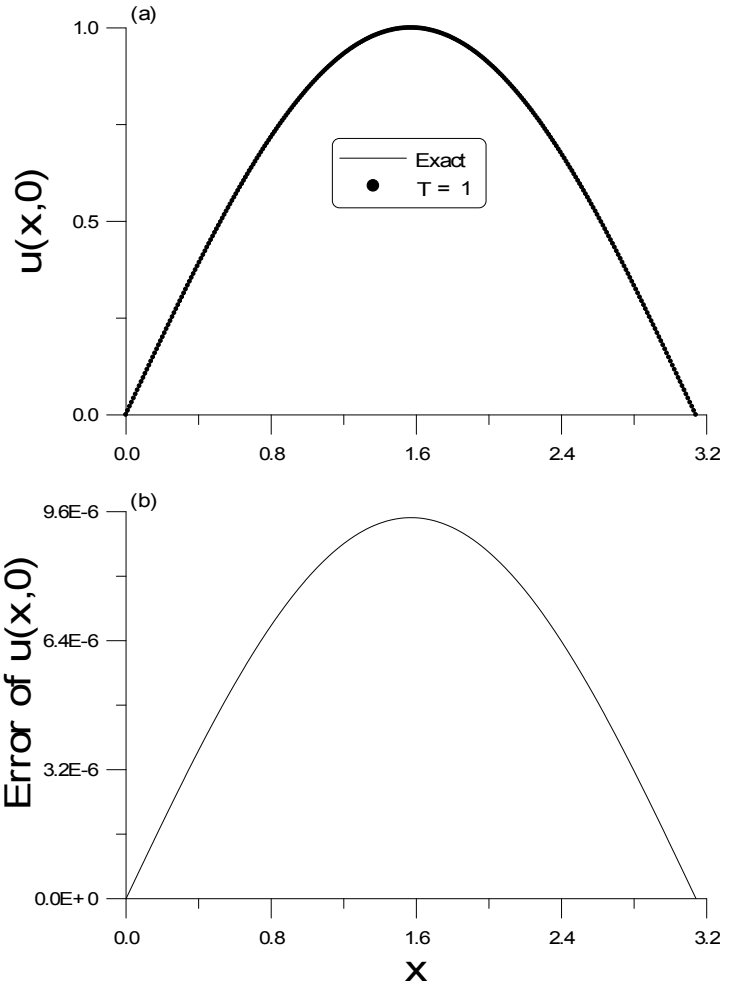

Figure 10: Comparisons of the exact solutions and numerical solutions with the final time $T = 1$, and the corresponding numerical errors.

per), and in [Nam (2010)] with that from the truncation method (see Table 1 of the above cited paper), we can say that the BGPS does not need to use those complex procedures (e.g., the regularization technique, the method of integral equation) and still obtain good results. Besides, we give a more ill-posed example than the one above by employing the BGPS. Let $T = 7.5$. The final data are large and on the order of $O(10^3)$. In Fig. 11(b), the errors of numerical solutions calculated by BGPS with one step and $\Delta x = 1/40$, and note that the accuracy is the order of 10^{-3}.

We plotted the numerical result with adding a relative noise with level $s_r = 0.1\%$ on the input final data in Fig. 12(a) by the dotted line. Note that the accuracy is still better than the order of 10^{-2} even under a disturbance.

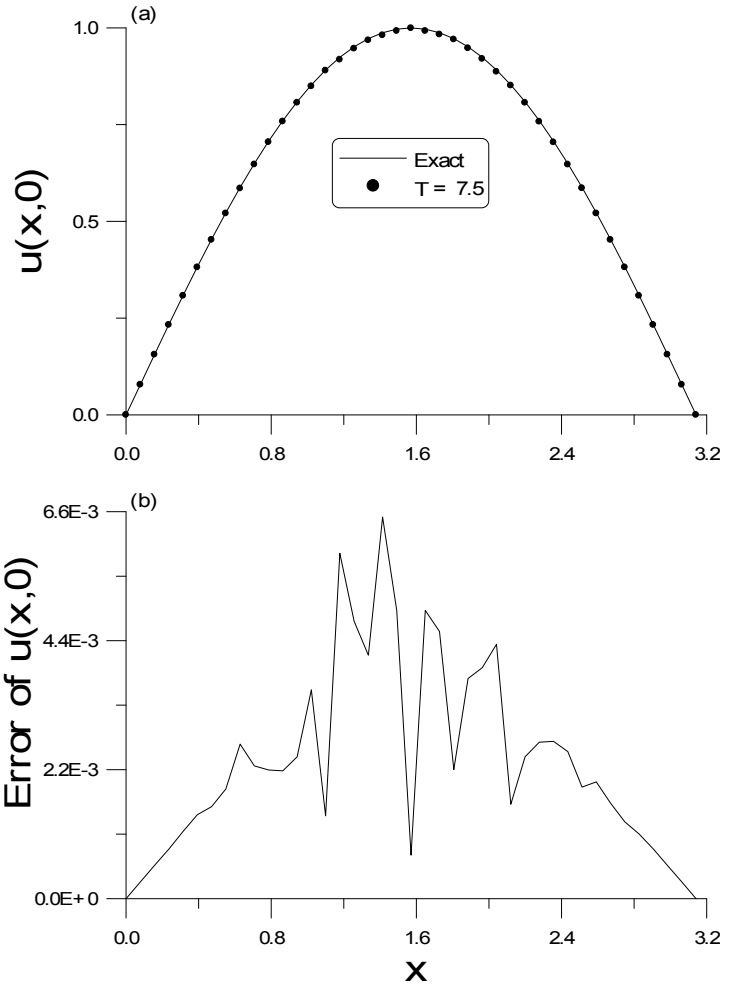

Figure 11: Comparisons of the exact solutions and numerical solutions with the final time $T = 7.5$, and the corresponding numerical errors.

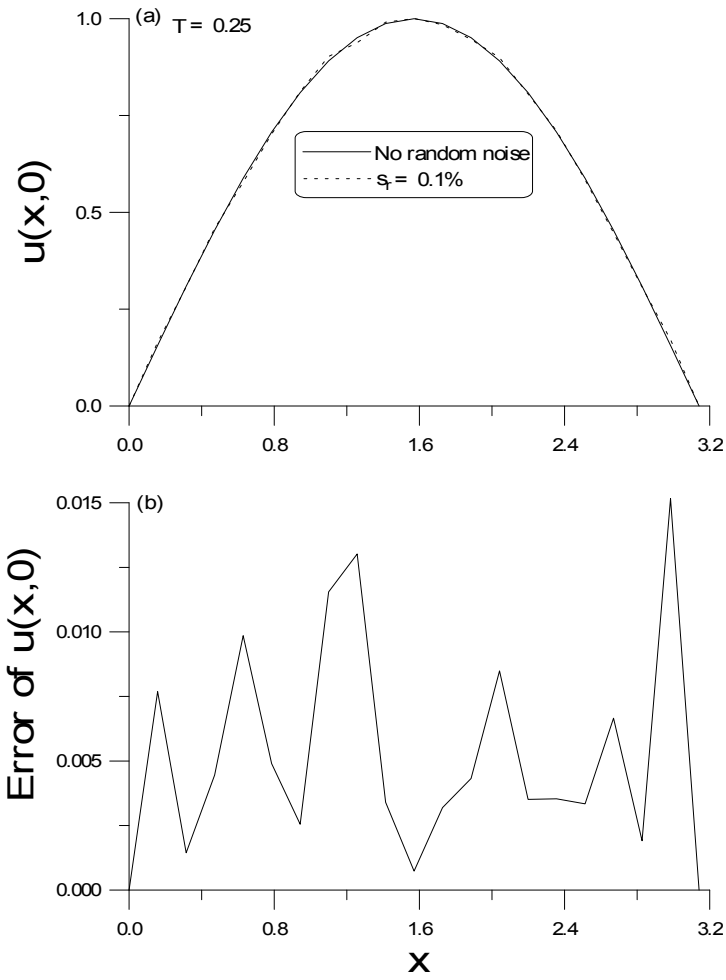

Figure 12: Comparisons of numerical solutions were made in (a) with different levels of noise s_r = 0, 0.1%, and (b) the corresponding numerical errors.

4.6 Example 6

Let us consider the two-dimensional nonhomogeneous BHCP:

$$u_t = u_{xx} + u_{yy} + 3e^t sin(x) sin(y),\ 0 < x < \pi, 0 < y < \pi, 0 < t < T, \tag{54}$$

with the boundary conditions

$$u(0,y,t) = u(\pi,y,t) = u(x,0,t) = u(x,\pi,t) = 0, \tag{55}$$

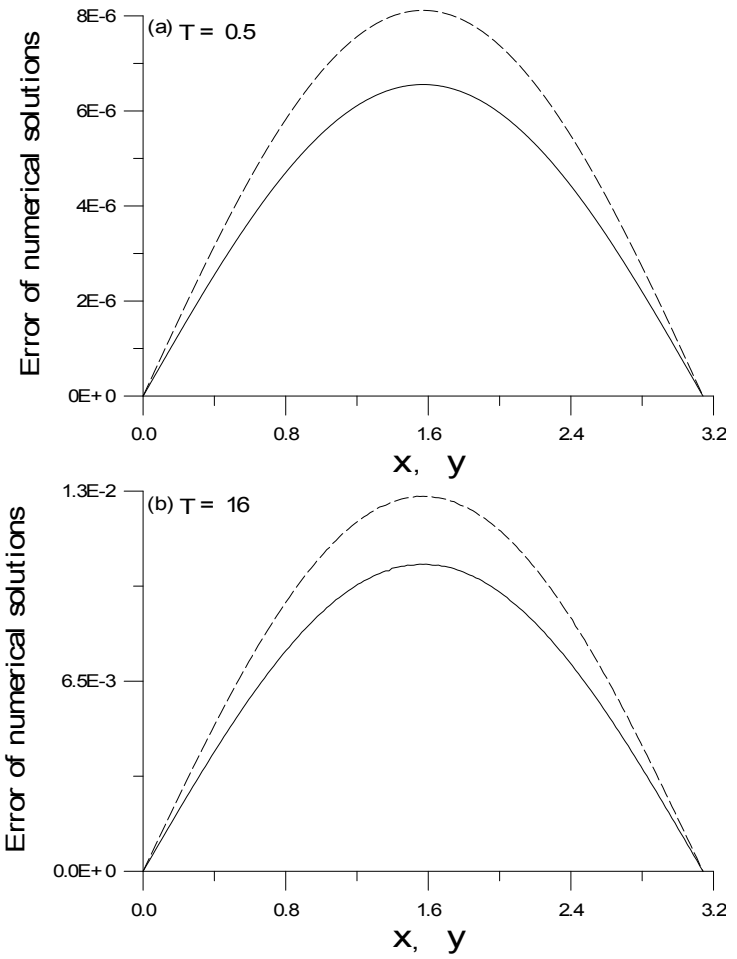

Figure 13: The errors of BGPS solutions for Example 6 are plotted in (a) with $T = 0.5$, and in (b) with $T = 16$.

and the final time condition

$$u(x,y,T) = e^{\mathrm{T}} sin(x) sin(y). \tag{56}$$

The exact solution is given by

$$u(x,y,t) = e^{t} sin(x) sin(y). \tag{57}$$

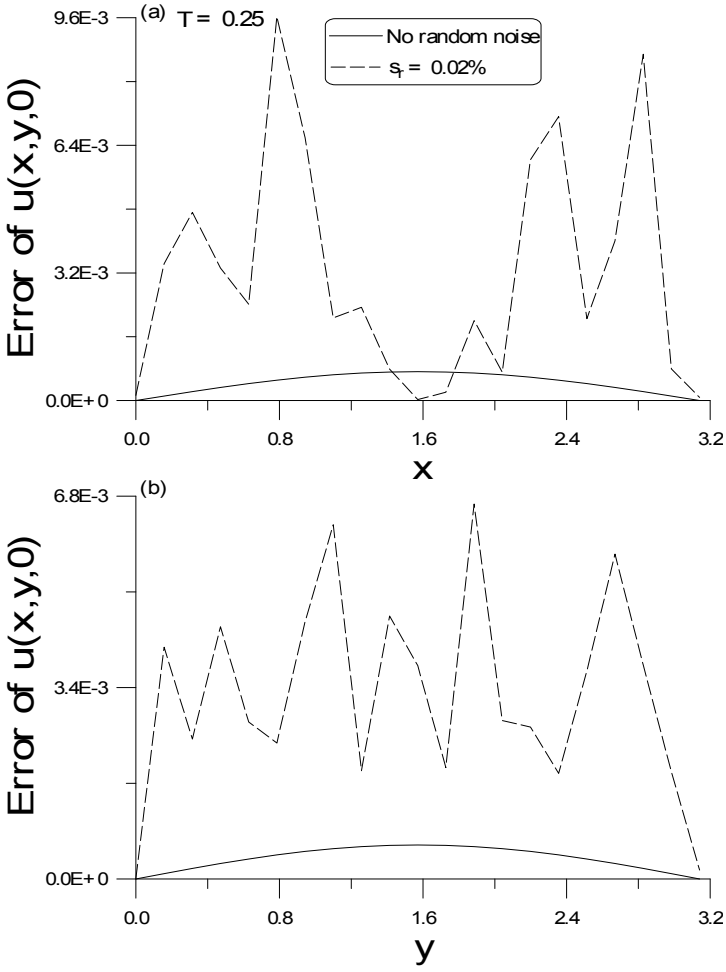

Figure 14: The numerical errors of BGPS solutions with and without random noise effect for Example 6 are plotted in (a) with respect to x at fixed $y = \pi/3$, and in (b) with respect to y at fixed $x = \pi/4$.

Fig. 13(a) indicates the errors of numerical solutions obtained from the BGPS for the case of $T = 0.5$ where the grid lengths $\Delta x = \Delta y = \pi/295$ and the time stepsize $\Delta t = 0.5$. At the point $x = 72\pi/295$, the error is plotted with respect to y by a dashed line, and at the point $y = 97\pi/295$, the error is plotted with respect to x by a solid line. The latter one is smaller than the former one because the point $y = 97\pi/295$ is near the boundary. However, the errors are smaller than that calculated by Tuan and Trong (2009) as shown in Table 1 therein.

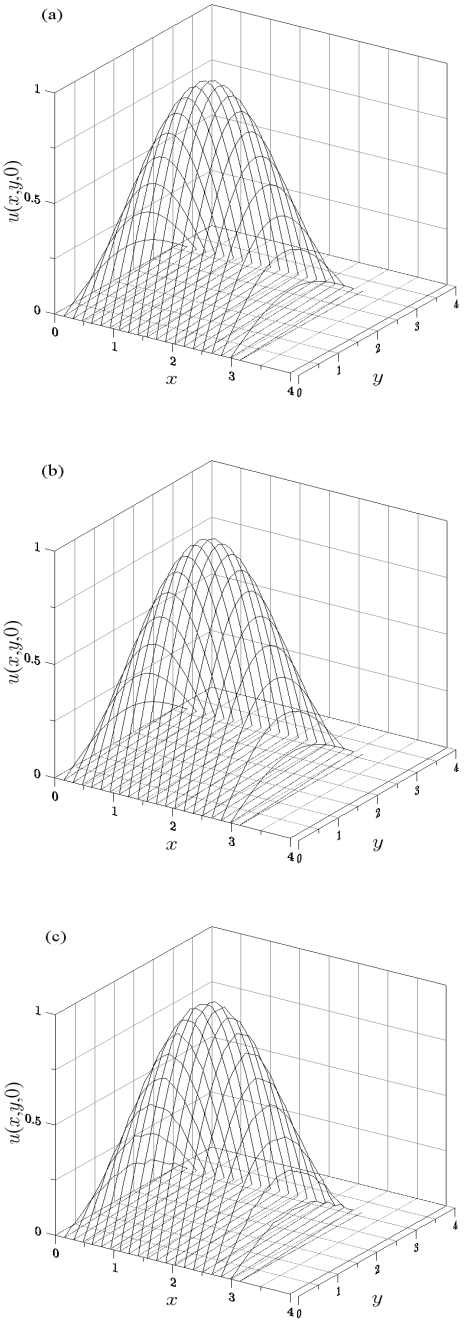

Figure 15: The exact solution for Example 6 of two-dimensional nonhomogeneous BHCP with $T = 0.25$ are shown in (a), in (b) the BGPS solution without random noise effect, and in (c) the FTIM solution with random noise.

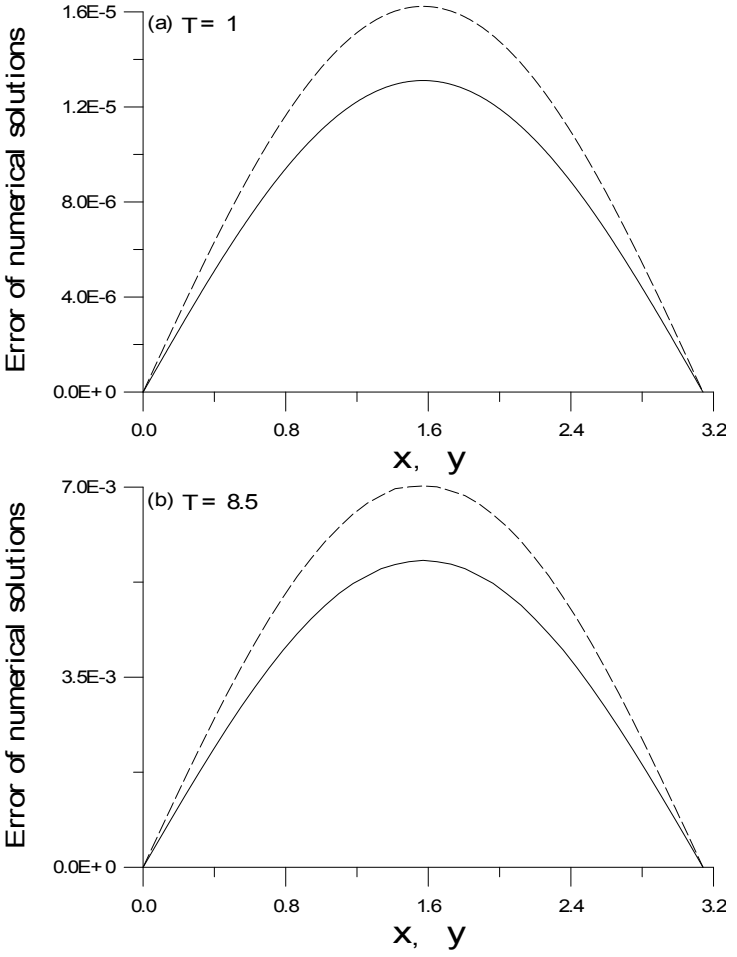

Figure 16: The errors of BGPS solutions for Example 7 are plotted in (a) with T = 1, and in (b) with T = 8.5.

To give a stringent test of the BGPS when applied the BGPS to this example, we let T = 16, and the final data is very large in the order of $O(10^7)$. However, we can use the BGPS to retrieve the desired initial data $\sin\beta x \sin\beta y$, which is in the order of $O(1)$. The errors of numerical solutions calculated by the BGPS with $\Delta x = \Delta y = \pi/180$ and one step in the calculation are shown in Fig. 13(b), where at the point $x = 44\pi/180$, the error is plotted with respect to y by a dashed line, and at the point $y = 58\pi/180$, the error is plotted with respect to x by a solid line. For

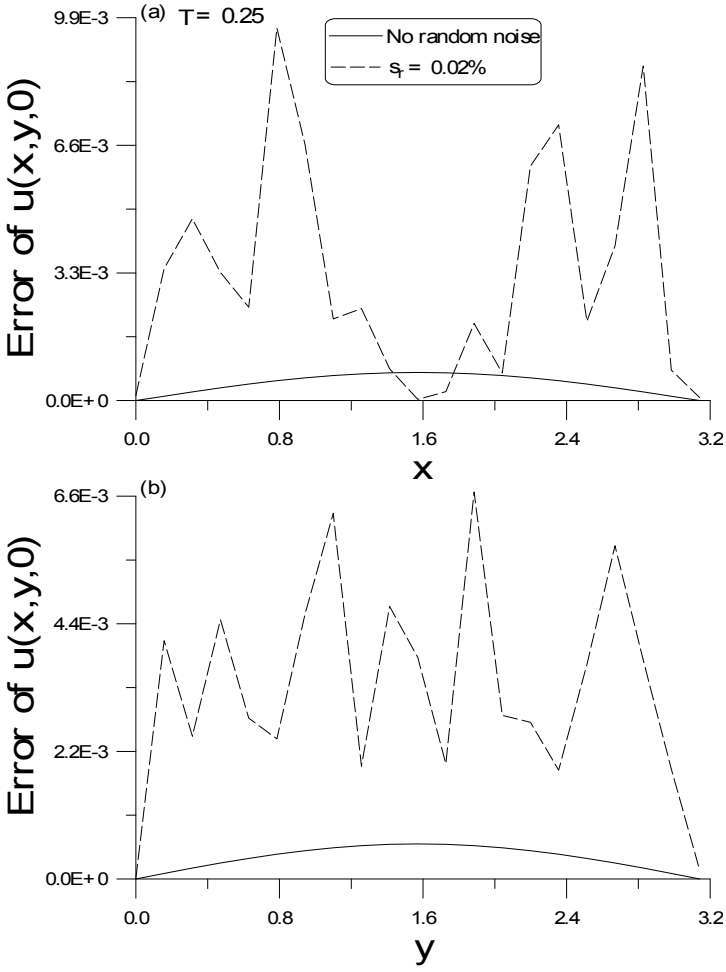

Figure 17: The numerical errors of BGPS solutions with and without random noise effect for Example 7 are plotted in (a) with respect to x at fixed $y = \pi/3$, and in (b) with respect to y at fixed $x = \pi/4$.

this very difficult problem, the BGPS proposed here is also good with a maximum error 1.28×10^{-2}.

In Fig. 14, we compare the numerical errors with $T = 0.25$ for two cases: one without the random noise and the other with the relative random noise in the level of $s_r = 0.02\%$. The exact solutions and numerical solutions are plotted in Figs. 15(a)-(c) sequentially. Even under the noise, the numerical solution displayed in

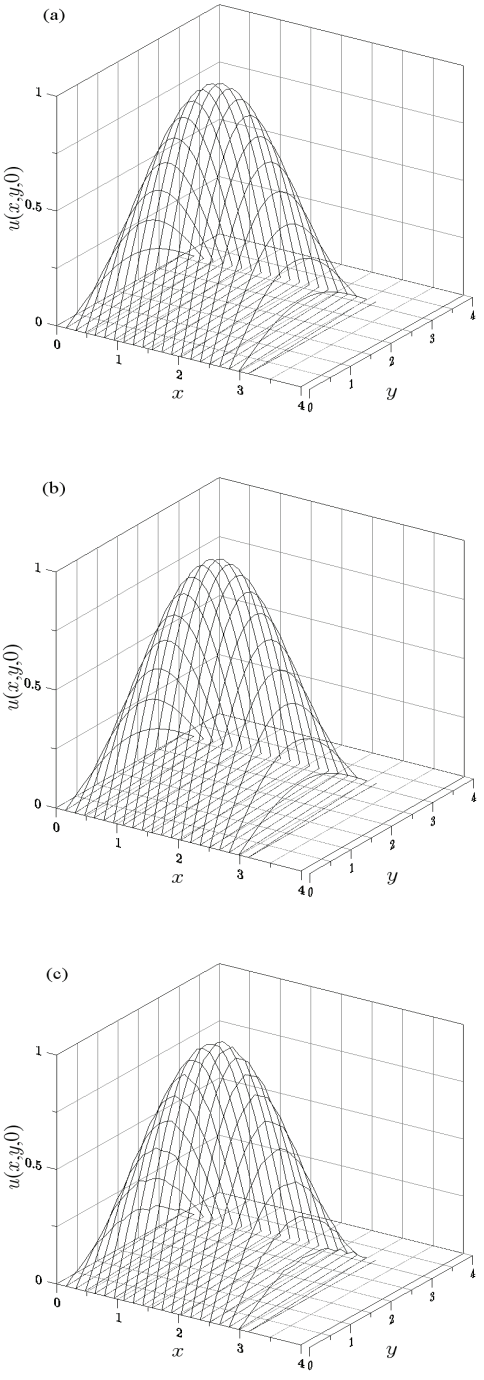

Figure 18: The exact solution for Example 7 of two-dimensional nonlinear BHCP with $T = 0.25$ are shown in (a), in (b) the BGPS solution without random noise effect, and in (c) the BGPS solution with random noise.

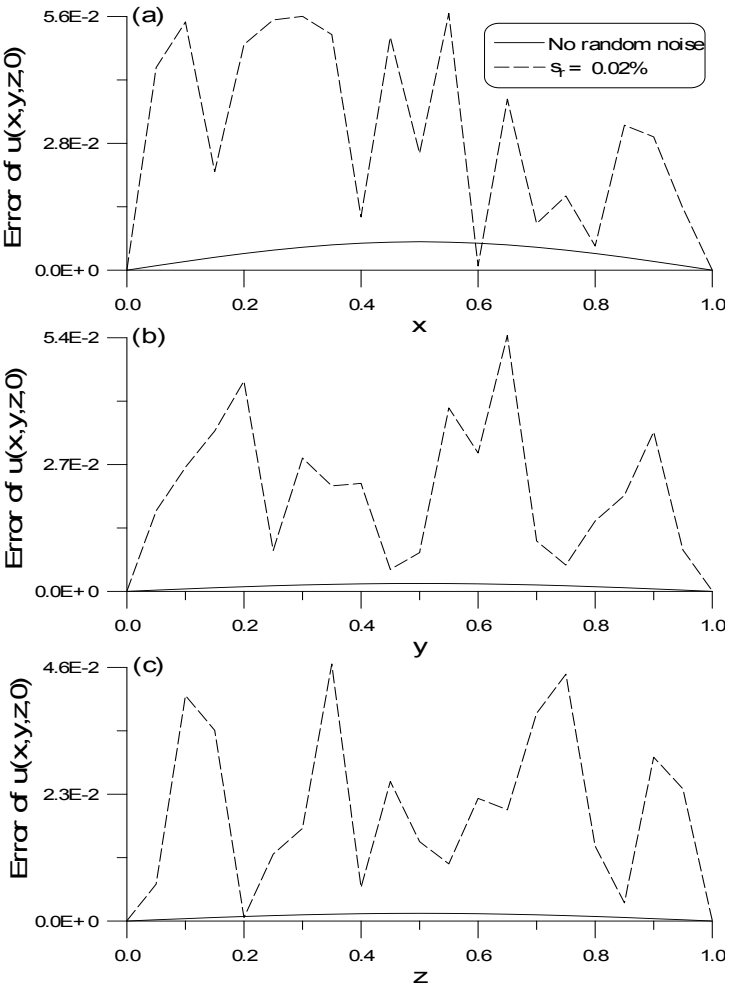

Figure 19: The numerical errors of BGPS solutions with and without random noise effect for Example 8 are plotted in (a) with respect to x at fixed $y = 0.3$ and $z = 0.8$, (b) with respect to y at fixed $x = 0.1$ and $z = 0.8$, and (a) with respect to z at fixed $x = 0.1$ and $y = 0.3$.

Fig. 15(c) is a good approximation to the exact initial data as shown in Fig. 15(a).

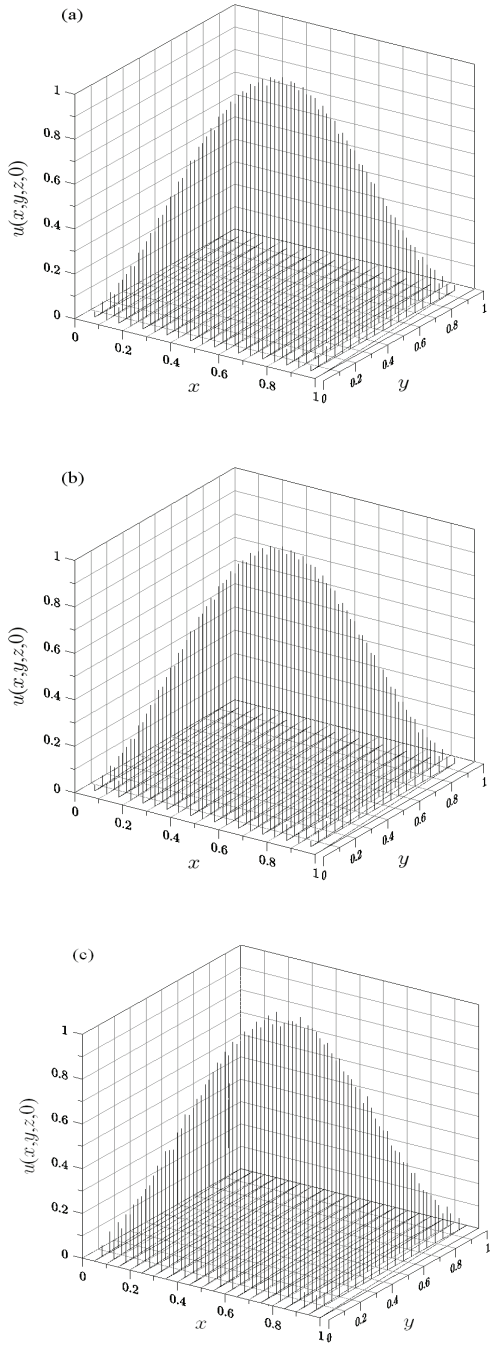

Figure 20: The exact solution for Example 8 of three-dimensional nonhomogeneous BHCP with $T = 0.25$ are shown in (a), in (b) the BGPS solution without random noise effect, and in (c) the BGPS solution with random noise.

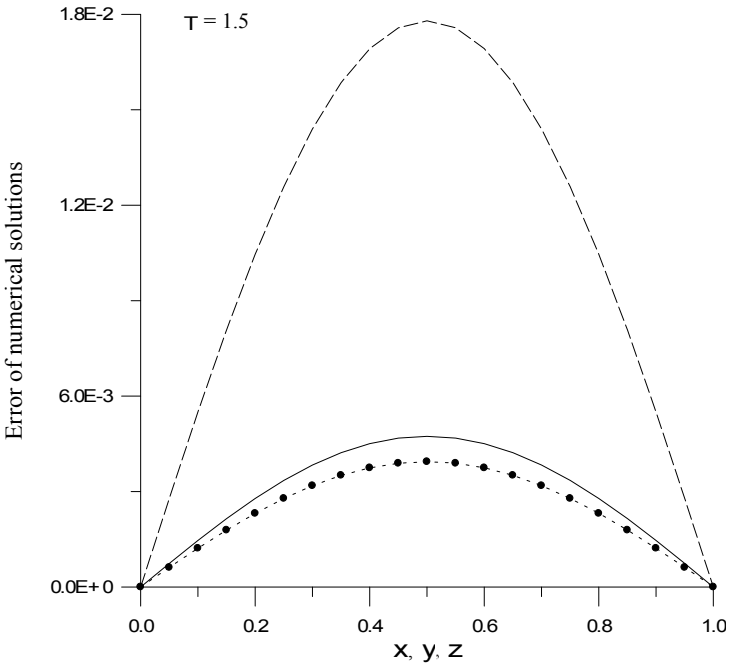

Figure 21: The errors of BGPS solutions for Example 8 with $T = 1.5$.

4.7 Example 7

Let us then consider the simple two-dimensional Allen-Cahn equation:

$$u_t = u_{xx} + u_{yy} + u - u^3 + 2e^t sin(x)sin(y) + e^{3t} sin^3(x)sin^3(y),\ 0 < x < \pi,\ 0 < y < \pi,\ 0 < t < T, \tag{58}$$

with the boundary conditions

$$u(0,y,t) = u(\pi,y,t) = u(x,0,t) = u(x,\pi,t) = 0, \tag{59}$$

and the final time condition

$$u(x,y,T) = e^{\mathrm{T}} sin(x)sin(y). \tag{60}$$

The exact solution is given by

$$u(x,y,t) = e^t sin(x)sin(y). \tag{61}$$

Fig. 16(a) indicates the errors of numerical solutions obtained from the BGPS for the case of $T = 1$ where the grid lengths $\Delta x = \Delta y = \pi/295$ and the time stepsize $\Delta t = 1$. At the point $x = 72\pi/295$, the error is plotted with respect to y by a dashed line, and at the point $y = 97\pi/295$, the error is plotted with respect to x by a solid line. The latter one is smaller than the former one because the point $y = 97\pi/295$, is near the boundary. Furthermore, the errors are much smaller than that calculated by Trong and Tuan (2009b) as shown in Table therein.

When applied the BGPS to this instance, we give a strict test of the BGPS, let T = 8.5, and the final data is large in the order of $O(10^4)$. Nevertheless, we can use the BGPS to retrieve the desired initial data sin$x$sin$y$, which is in the order of $O(1)$. The errors of numerical solutions calculated by the BGPS with $\Delta x = \Delta y = \pi/40$ and one step in the calculation are shown in Fig. 16(b), where at the point $x = 9\pi/40$, the error is plotted with respect to y by a dashed line, and at the point $y = 12\pi/40$, the error is plotted with respect to x by a solid line. For this very difficult problem, the BGPS proposed here is also good with a maximum error 7×10^{-3}.

In Fig. 17, we compare the numerical errors with T = 0.25 for two cases: one without the random noise and the other with the relative random noise in the level of s_r = 0.02%. The exact solutions and numerical solutions are plotted in Figs. 18(a)-(c) sequentially. Even under the noise, the numerical solution displayed in Fig. 18(c) is a good approximation to the exact initial data as presented in Fig. 18(a).

4.8 Example 8

Let us consider a three-dimensional nonhomogeneous BHCP:

$$u_t = u_{xx} + u_{yy} + u_{zz} + 4\pi^2 e^{\pi^2 t} sin(\pi x) sin(\pi y) sin(\pi z), \\ 0 < x < 1, 0 < y < 1, 0 < z < 1, 0 < t < 1, \quad (62)$$

with the boundary conditions

$$u(0,y,z,t) = u(1,y,z,t) = u(x,0,z,t) = u(x,1,z,t) = u(x,y,0,t) = u(x,y,1,t) = 0, \quad (63)$$

and the final time condition

$$u(x,y,z,T) = e^{\pi^2 T} sin(\pi x) sin(\pi y) sin(\pi z). \quad (64)$$

The exact solution is given by

$$u(x,y,z,t) = e^{\pi^2 t} sin(\pi x) sin(\pi y) sin(\pi z). \quad (65)$$

In Fig. 19, we compare the numerical errors with $T = 0.25$ for two cases: one without the random noise and the other with the relative random noise in the level of $s_r = 0.02\%$. The exact solutions and numerical solutions are plotted in Figs. 20(a)-(c) sequentially. Even under the noise, the numerical solution displayed in Fig. 20(c) is a good approximation to the exact initial data as displayed in Fig. 20(a).

In Fig. 21, we compare the numerical errors with $T = 1.5$, where the grid lengths are taken to be $\Delta x = \Delta y = \Delta z = 1/20$, the time stepsize is taken to be $\Delta t = 1.5$. At the point $x = 0.1$ the error is plotted with respect to y and z by a dashed line, at the point $y = 0.3$ the error is plotted with respect to x and z by a solid line, and at the point $z = 0.8$ the error is plotted with respect to x and y by a dotted line. The latter one is smaller than the former two because the point $z = 0.8$ is near the boundary. This example is a hard BHCP problem to test the numerical performance of novel numerical approaches. Nevertheless, to the authors' best knowledge, there has been no report that numerical approaches can calculate this ill-posed multi-dimensional nonhomogeneous BHCP very well as our method.

5 Conclusions

The multi-dimensional nonlinear and nonhomogeneous BHCPs have been calculated by the formulation with a semi-discretization of the spatial coordinate of backward heat conduction equations in conjunction with the backward group preserving numerical integration scheme. In this paper, we are interested in this numerical integration problem, where the pivotal point is the establishment of a past cone and a BGPS. In addition, we can erect a past cone, Lie algebra and Lie group delineation of the backward problems governed by differential equations. Eight numerical examples of the multi-dimensional nonlinear and nonhomogeneous BHCP work, and we display, on the basis of those numerical instances, that the BGPS is applicable to the multi-dimensional nonlinear and nonhomogeneous BHCP, even for the very strongly ill-posed ones. The numerical errors of our approach are in the order of $O(10^{-3})$–$O(10^{-7})$. Under specific time stepsizes and grid spacing lengths, the BGPS can produce an accurate result, and the implementation is simple. Moreover, the efficiency of one-step BGPS is rooted in the closure property of the Lie group that we use it to construct the numerical method for the multi-dimensional nonlinear and nonhomogeneous BHCP.

References

Chang, C.-W.; Liu, C.-S.; Chang, J.-R. (2005): A group preserving scheme for inverse heat conduction problems. *CMES: Computer Modeling in Engineering &*

Sciences, vol. 10, pp. 13–38.

Chang, C.-W.; Liu, C.-S.; Chang, J.-R. (2009): A new shooting method for quasi-boundary regularization of multi-dimensional backward heat conduction problems. *J. Chinese Inst. Engineers*, vol. 32, pp. 307–318.

Chang, C.-W.; Liu, C.-S.; Chang, J.-R. (2010a): A quasi-boundary semi-analytical method for backward heat conduction problems. *J. Chinese Inst. Engineers*, vol. 33, pp. 163–175.

Chang, C.-W.; Liu, C.-S.; Chang, J.-R. (2010b): A quasi-boundary semi-analytical approach for two-dimensional backward heat conduction problems. *CMC: Computers, Materials & Continua*, vol. 15, pp. 45–66.

Chang, J.-R.; Liu, C.-S.; Chang, C.-W. (2007): A new shooting method for quasi-boundary regularization of backward heat conduction problems. *Int. J. Heat Mass Transfer*, vol. 50, pp. 2325–2332.

Chiwiacowsky, L. D.; de Campos Velho, H. F. (2003): Different approaches for the solution of a backward heat conduction problem. *Inv. Prob. Eng.*, vol. 11, pp. 471–494.

Feng, X.-L.; Qian, Z.; Fu, C.-L. (2008): Numerical approximation of solution of nonhomogeneous backward heat conduction problem in bounded region. *Math. Comp. Simul.*, vol. 79, pp. 177–188.

Han, H.; Ingham, D. B.; Yuan, Y. (1995): The boundary element method for the solution of the backward heat conduction equation. *J. Comp. Phys.*, vol. 116, pp. 292–299.

Iijima, K. (2004): Numerical solution of backward heat conduction problems by a high order lattice-free finite difference method. *J. Chinese Inst. Engineers*, vol. 27, pp. 611–620.

Jourhmane, M.; Mera, N. S. (2002): An iterative algorithm for the backward heat conduction problem based on variable relaxation factors. *Inv. Prob. Eng.*, vol. 10, pp. 293–308.

Kirkup, S. M.; Wadsworth, M. (2002): Solution of inverse diffusion problems by operator-splitting methods. *Appl. Math. Model.*, vol. 26, pp. 1003–1018.

Lesnic, D.; Elliott, L.; Ingham, D. B. (1998): An iterative boundary element method for solving the backward heat conduction problem using an elliptic approximation. *Inv. Prob. Eng.*, vol. 6, pp. 255–279.

Li, H.; Liu, J. J. (2005): Solution of Backward Heat Problem by Morozov Discrepancy Principle and Conditional Stability. *Num. Math. J. of Chinese Univ.*, vol. 14, pp. 180–192.

Liu, C.-S. (2001): Cone of non-linear dynamical system and group preserving

schemes. *Int. J. of Non-Linear Mech.*, vol. 36, pp. 1047–1068.

Liu, C.-S. (2004): Group preserving scheme for backward heat conduction problems. *Int. J. Heat Mass Transfer*, vol. 47, pp. 2567–2576.

Liu, C.-S. (2006): An efficient backward group preserving scheme for the backward in time Burgers equation. *CMES: Computer Modeling in Engineering & Sciences*, vol. 12, pp. 55–65.

Liu, C.-S.; Chang, C.-W.; Chang, J.-R. (2006): Past cone dynamics and backward group preserving schemes for backward heat conduction problems. *CMES: Computer Modeling in Engineering & Sciences*, vol. 12, pp. 67–81.

Liu, C.-S.; Chang, C.-W.; Chang, J.-R. (2010): The backward group preserving scheme for 1D backward in time advection-dispersion equation. *Num. Meth. Partial Diff. Eq.*, vol. 26, pp. 61–80.

Liu, J. (2002): Numerical solution of forward and backward problem for 2-D heat conduction equation. *J. Comp. Appl. Math.*, vol. 145, pp. 459–482.

Long, N. T.; Dinh, A. P. N. (1994): Approximation of parabolic non-linear evolution equation backward in time. *Inv. Prob.*, vol. 10, pp. 905–914.

Mera, N. S. (2005): The method of fundamental solutions for the backward heat conduction problem. *Inv. Prob. Sci. Eng.*, vol. 13, pp. 65–78.

Mera, N. S.; Elliott, L.; Ingham, D. B.; Lesnic, D. (2001): An iterative boundary element method for solving the one-dimensional backward heat conduction problem. *Int. J. Heat Mass Transfer*, vol. 44, pp. 1937–1946.

Mera, N. S.; Elliott, L.; Ingham, D. B. (2002): An inversion method with decreasing regularization for the backward heat conduction problem. *Num. Heat Transfer B*, vol. 42, pp. 215–230.

Muniz, W. B.; Ramos, F. M.; de Campos Velho, H. F. (2000): Entropy- and Tikhonov-based regularization techniques applied to the backward heat equation. *Int. J. Comp. Math.*, vol. 40, pp. 1071–1084.

Muniz, W. B.; de Campos Velho, H. F.; Ramos, F. M. (1999): A comparison of some inverse methods for estimating the initial condition of the heat equation. *J. Comp. Appl. Math.*, vol. 103, pp. 145–163.

Nam, P. T. (2010): An approximate solution for nonlinear backward parabolic equations. *J. Math. Anal. Appl.*, doi:10.1016/j.jmaa.2010.01.020.

Trong, D. D.; Quan, P. H.; Khanh, T. V.; Tuan, N. H. (2007): A nonlinear case of the 1-D backward heat problem: Regularization and error estimate. *Zeitschrift Anal. und ihre*, vol. 26, pp. 231–245.

Trong, D. D.; Tuan, N. H. (2006): Regularization and error estimates for nonho-

mogeneous backward heat problems. Electron. *J. Diff. Eq.*, vol. 2006, pp. 1–10.

Trong, D. D.; Tuan, N. H. (2008a): A nonhomogeneous backward heat problem: regularization and error estimates. *Electron. J. Diff. Eq.*, vol. 2008, pp. 1–14.

Trong, D. D.; Tuan, N. H. (2008b): Stabilized quasi-reversibility method for a class of nonlinear ill-posed problems. *Electron. J. Diff. Eq.*, vol. 2008, pp. 1–12.

Trong, D. D.; Tuan, N. H. (2009a): Regularization and error estimate for the nonlinear backward heat problem using a method of integral equation. *Nonlinear Anal.*, vol. 71, pp. 4167–4176.

Trong, D. D.; Tuan, N. H. (2009b): Remarks on a 2-D nonlinear backward heat problem using a truncated Fourier series method. *Electron. J. Diff. Eq.*, vol. 2009, pp. 1–13.

Tuan, N. H.; Trong, D. D. (2009): A new regularized method for two dimensional nonhomogeneous backward heat problem. *Appl. Math. Comp.*, vol. 2008, pp. 1–14.